EXPERIMENTAL STUDY ON SEISMIC SHEAR AMPLIFICATION IN WALLS WITH DISCONTINUITIES

F. Jiménez[1] and L. M. Massone[2]
[1] M.Sc., Department of Civil engineering, Universidad de Chile, fjimenez@ing.uchile.cl
[2] Associate Professor, Department of Civil engineering, Universidad de Chile, lmassone@ing.uchile.cl

Abstract

RC structural slender walls under large seismic excitation are expected to behave nonlinear due to yielding of the longitudinal reinforcement, which produces plastic hinges usually at the base of the structure. This occurs due to the fact that design uses reduced forces when the response is compared with linear models for an earthquake or spectra. It is common that the base moment reaches its capacity mainly affected by the first vibration mode. However, the base shear could be affected by the higher modes once yielding in flexure has occurred, which might lead that the base shear is underestimated. This phenomenon is known as dynamic shear amplification, which is not incorporated in the Chilean design code. To investigate shear demand due to higher modes, an experimental program is accomplished on five test specimens 1:10 scaled. The test program considered cantilever RC shear wall with rectangular cross section and a total mass of 1 ton, lumped at 5 levels. All five specimens considered discontinuities common in construction and were only defined at the base of the specimens (door opening, setback) and 1 specimen did not consider shear reinforcement or boundary detailing. They are mounted on a unidirectional shaking table to impose seismic input. The specimens are 2.15 m high, 15 cm long and 4 cm thick. The tests are performed to archive nonlinear effects and higher mode excitation in order to study dynamic non-linear shear amplification. Indeed, experimental data of the phenomenon is obtained for walls built according to local practice, and results from a base wall is compared with wall with discontinuities that presented problems for the 2010 Chile earthquake, checking the amplification impact in these structures. Specimens are tested with a generated synthetic signal based on the Constitution record from 2010 Chile earthquake scaled in time, as well as the Llolleo record from the 1985 Chile earthquake. All specimens are tested under incremental ground synthetic (Constitution) record scaling the acceleration from 10% to 200% of the base earthquake, and also with the Llolleo record scaled by 100% and 150%, when possible. Damage is concentrated at the wall base for all specimens; primary due to flexure with some participation of shear. For the synthetic record an average amplification of 1.3 is obtained, and a decrease in height of the resultant equivalent lateral force closes to $0.4h_w$. By increasing the intensity of the input record, amplification grows to an average of 1.8. While it decreases drastically when subjected to input records with low frequency content (Llolleo). No significant difference is observed in shear amplification with specimens with a base central opening, nor with the flag wall, even though the cracking and failure mode was different for such specimens. Ductility demand shows no correlation when 2 different earthquakes are considered, whereas the frequency content and Arias intensity (Ia) of the input record directly affected the shear amplification.

Keywords: slender wall; discontinuities; higher modes; shear amplification.

1. Introduction

On February 27, 2010 (27F) Chile was affected by a Mw 8.8 earthquake in the south-central area. The damage observed in reinforced concrete (RC) structures was due mainly to base moment and axial load, which resulted in concrete crushing and buckling of steel bars by poor detailing of boundary elements in walls. Although damage was primary caused due to poor detailing, large axial loads and frequently discontinuities also affected the structural behavior. A typical discontinuity in Chilean construction is the result of the architectural requirements, where the lower floors (typically for parking) are shorter in length than the upper floors (setback or flag-walls); and walls with openings, primarily by gateways. The seismic event resulted in the modification of the concrete Chilean code, but the focus was on the flexural and axial damage, so that discontinuities were not considered. Furthermore, by providing a better detailing, and therefore flexural ductility, the walls are more susceptible to brittle shear failure, if the dynamic response is not well understood.

One of the phenomena associated with shear is the dynamic amplification. Shear amplification take place when base shear increases due to high modes, especially when the wall reaches the nonlinear range. This plasticization commonly develops at the wall base, which is affected largely by the first mode, leaving higher modes nearly intact, and increasing their participation after flexural yielding, causing a resultant equivalent lateral force applied at a lower lever with a higher magnitude (base shear) since the maximum base moment remains almost constant (see Fig. 1).

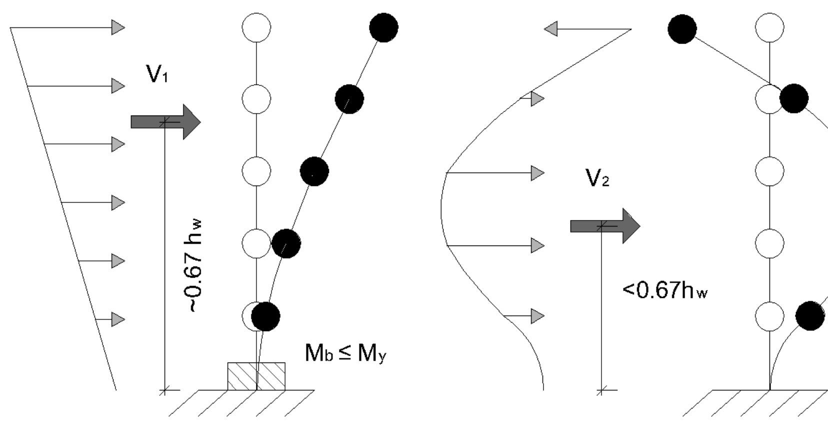

Fig. 1 – Equivalent lateral forces in cantilever wall for the first two modes.

Shear amplification has been studied since the 70's, when Blakeley [1] proposed amplification formulation for New Zealand code [2] that increases as a function of the number of stores. Derecho [3] and others [4, 5] demonstrate that shear at base increases with ductility demand. Those mentioned author, as same as many researches, have reached conclusions based on nonlinear time-history models using suites of records, whereas a theoretical formulation was given by Eibl and Keintzel [6], and Keintzel [7]. Lately extensions and corrections were proposed [8, 9], as summarized by Rutemberg [10]. Besides, dynamic shear amplification has been observed in experimental tests as well. Panagiotou and Restrepo [11] observed a moment base overstrength, defined as the ratio of maximum measured base moment and the design base moment, of 2.71; while shear base overstrength factor observed was 4.20, yielding in an increase of 1.5 times more for shear. Also Ghorbanirenani et al. [12] recorded a shear amplification factor of 2.2 in their test. Both test programs have been reproduced numerically [13, 14]. Very recently Isakovic et al. [15], in a parametric non-linear study of coupled walls with one row of openings, conclude that in this case it is conservative to use expressions for cantilever walls.

Different shear amplification factors are used in design codes. Amplification in New Zealand code depends on the number of stores; while Eurocode 8 formulation requires moment resistance, period, ductility and response spectrum shape. On the other hand, it is absent in the ACI-318, Chilean code and other current codes.

In order to investigate the impact of dynamic shear amplification in Chilean construction an experimental program that consists of five RC walls specimens at 1:10 scale is performed. Test take place in a unidirectional shake table, in the structural dynamic laboratory at the University of Chile. Models are constructed as a cantilever, with masses lumped at 5 stories.

2. Experimental Program

2.1 General Considerations and Scale Factors

The prototype wall corresponds to a wall designed according to Chilean code [16, 17] and ACI-318 [18] code. It is located according to Chilean code in seismic zone 3 and soil type C, which corresponds to a PGA = 0.4g and a soil with shear velocity between 350 to 500 m/s. The thickness is 40 cm, and the length of (l_w) 1.5 m is limited for a minimum length to cross-section ratio of 3. Total height (h_w) is 21.5 m (h_w/l_w ~ 14) distributed in 8 levels, with a 2.7 m story high. The total mass is 100 ton. Nominal compressive concrete strength is f'_c = 25 MPa, resulting in an axial force of $0.07A_gf'_c$, which is relatively low for local practice. Fundamental period, considering the uncracked section, is 1.12 s; higher than average for 8-story flexible structures, for which is 0.53 s, according local configurations [19], however observable on rare occasions in the same research. Incorporation of discontinuities considered: lengthening of 20% above the wall base - flag wall (M2), a central opening at base with a short span of 10% of total length (M3), and a central opening with an span of 30% of total length (M4).

The distance scale factor used is l_r = 0.1 and the scale method used is the described by Carvalho [20] in which simultaneously fulfill the Froude and Cauchy laws for dynamic analysis. Among other parameters to scale, there is a time scale t_r = 0.316, while acceleration, strain and stress being equal to a factor of 1.

2.2 Design and Properties of the Test Specimens

2.2.1 Materials

Concrete used corresponds to a dry pre-mixed, in which the nominal maximum size of aggregates is 2.5 mm. Water/cement (W/C) ratio of 0.26 is used, and a plasticizer is used in a weight ratio of 0.78% to avoid concrete vibration. The average strength at the end of the tests is 42 MPa.

Longitudinal steel bars used have a local steel classification called A440-280H, these are plain bars of 6 mm diameter, with a tested yield stress of f_y = 387 MPa and tested maximum strength stress of f_u = 556 MPa. Steel for shear reinforcement bars and hoops is classified as AT56-50H with a bars diameter of 4 mm, a tested yield stress of f_y = 487 MPa and a tested ultimate strength of f_u = 685 MPa.

2.2.2 Specimen Design

Final design of walls is presented in Fig. 2. All walls are 4 cm thick and 2.15 m high. Walls M1 (base wall), M3, M4 and M5 are 15 cm long, while M2 is 15 cm at base (first 10 cm) and 18 cm long in the remaining height, i.e. 20% lengthened. Wall M3 has an opening of 10 cm in height and 1.5 cm in length (10% of total length), and wall M4 has an opening of the same height and 4.5 cm in length (30% of total length). Wall M5 is equal to wall M1, but without shear reinforcement or hoops. All walls have 2 longitudinal bars bonded at each boundary, and 2 longitudinal bars debonded (greased and covered) at the inside side of the boundary, which do not work in flexure, but contribute helping installing hoops for boundary detailing, except with wall M5 which has only bonded bars at each end because hoops are not used.

Each wall has two holes placed horizontally and spaced at 10 cm throughout five levels, where bars are placed to set metal plates that provide the required mass and axial load. The foundation of each specimen is 20 cm height, 30 cm wide and 45 cm long.

The design of the specimen tried to maintain most of the static and dynamic features invariants for different specimens. Considering tested material capacities, moment capacity at the wall base is M_n = 3.47 kNm, base yield moment is M_y = 3.24 kNm and base yield curvature is φ_y = 0.021 1/m and are equal for all the specimens under study. Moment capacity is calculate according ACI318-08 code and is designed for be reached while test is performed. Yield properties are calculated with a nonlinear fiber model, defined with usual material properties [21, 22]. The shear strength for walls according failure pattern (traditional value in brackets if corresponds) M1 and M2 is 12.3 kN, for M3 and M4 is 9.1 kN (11.7 and 10.4 respectively), and M5 is 6.1 kN according to ACI318-08. The nominal fundamental and second mode period are T_1 = 0.37 s, and T_2 = 0.06 s, for walls M1, M3, M4 y M5, whereas for wall M2 these are T_1 = 0.30 s, and T_2 = 0.05 s.

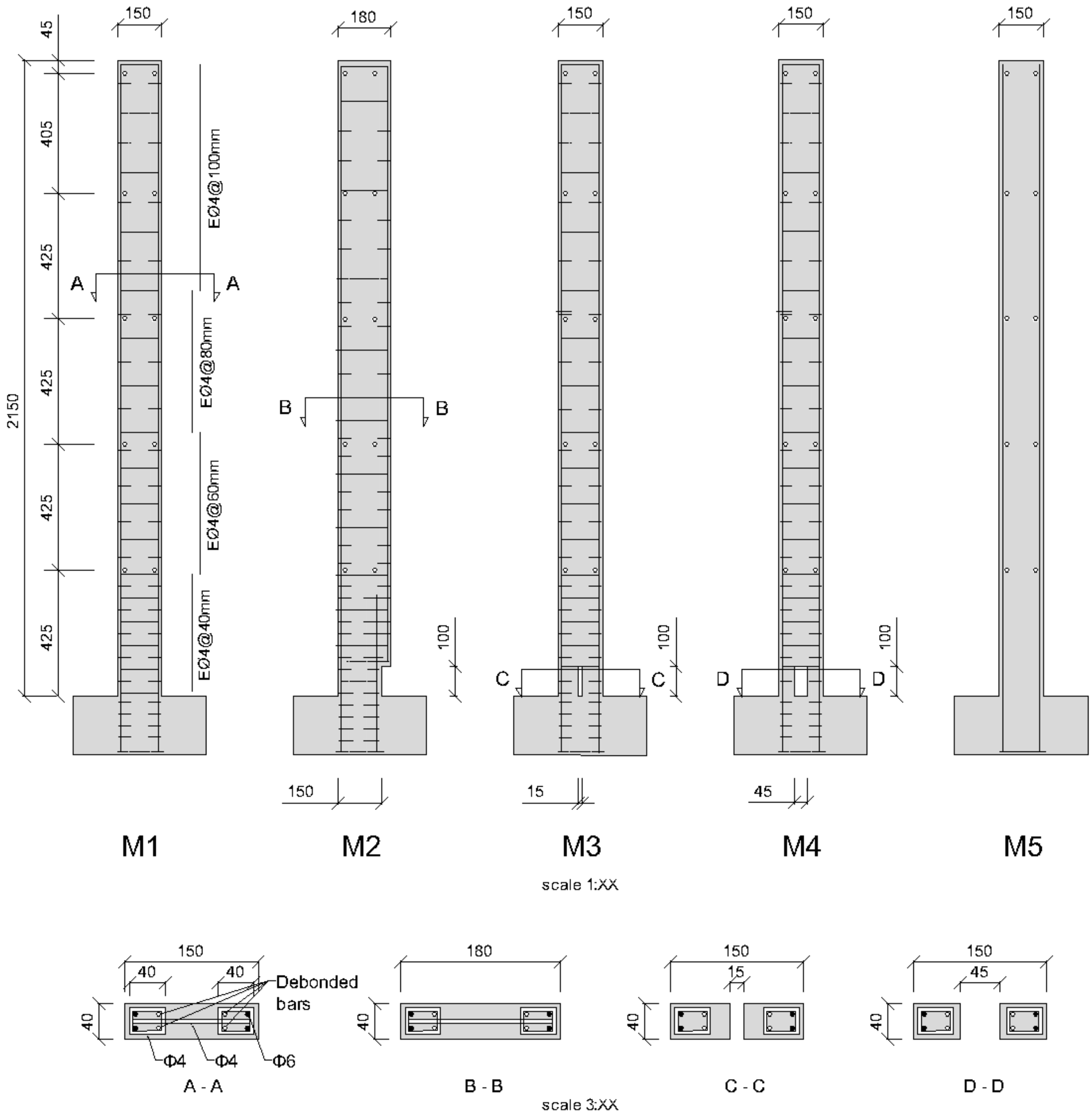

Fig. 2 – Wall and steel reinforcement detailing (dimensions in mm – section not to scale).

3. Input Ground Acceleration

Two input ground motion records are considered. One is a synthetic record based on Constitution record from the 2010 Chile earthquake. The time is scaled at t_r = .0.316 to be consistent with the scale laws considered [20]. This time scaling results in a pronounced peak in acceleration spectrum at 0.12 s, and variation of structure period within different walls could result in different results. Thus, the synthetic record is manipulated to smooth this behavior. Also, Llolleo record from the 1985 Chile earthquake is used without any scale. Displacement spectra and acceleration pseudo-spectra obtained from tests are shown in Fig. 3 (acceleration is scaled to compare input with different PGA). The specimens are subjected to forcing actions, scaled in acceleration, in the following sequence: synthetic Constitución (C) scale to 10% (C010), 100% (C100), 130% (C130), 150% (C150) and 200% (C200), and when possible to the Llolleo record scaled to 100% (L100) and 150% (L150).

(a) (b)

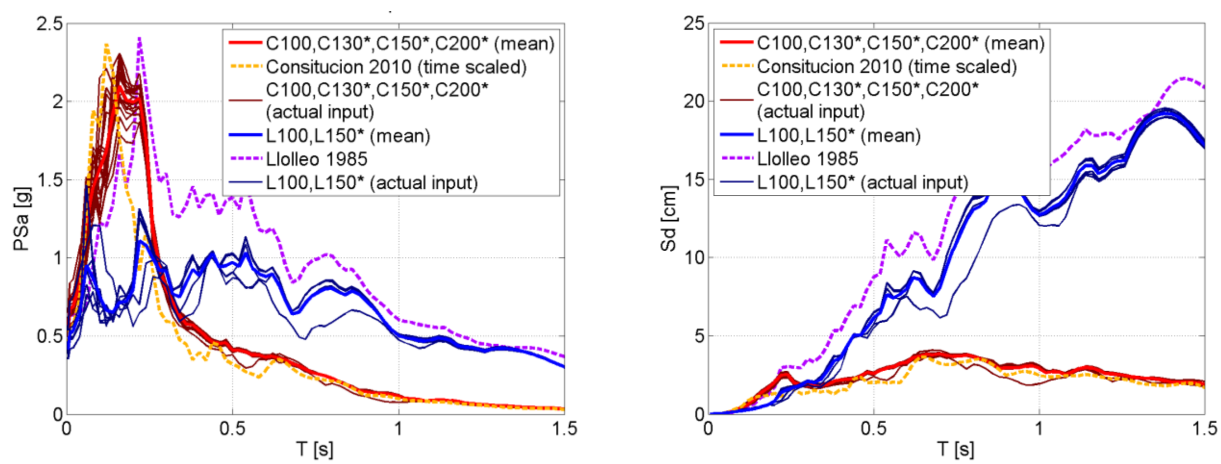

Fig. 3 – Actual input record - (a) Pseudo Acceleration Spectra and (b) Displacement Spectra. *: scaled in acceleration to compare with 100% scaled input acceleration.

4. Construction, Test set up and Instrumentation

Design was performed according ACI-318 and Chilean code provisions. In order to accomplish that, boundary elements were detailed with stirrups spaced at $6d_b$, i.e., ϕ4 mm hoops spaced at 40 mm at the wall plastic hinge region (base). Also, longitudinal bars anchored within the foundation have 90° hook and were extended 15 cm inside in order to provide adequate adherence. Despite the recommendations imposed by local regulations, due to scale limitations, a single layer of horizontal distributed reinforcement was placed. The foundation included 10 removable anchors attached to the base to prevent unwanted pedestal displacement or lifting. Concrete is placed in specimens entirely on the same day in two groups, first group includes M2, M3 and M5; and the second group includes M1 and M4; making sure that the composition and procedures are maintained. They cast horizontally, because of the difficulty of pouring concrete in a narrow element. Small size of aggregate (maximum size 2.5 mm) and a plasticizer is used for the same reason. Prior to test, the specimens are stored in a closed laboratory with curing for a few days.

50 steel plates are disposed in order to add inertial and axial force to specimens. Each plate weighs 19.7 kg. A steel structure supports laterally the walls (Fig. 4b), preventing movement out of the plane.

Instrumentation includes 6 unidirectional accelerometers EPISensor ES-U2 placed at each level (including the base) aligned to the movement of the shake table to capture inertial forces, which has an excellent match, in similar test [12], with the force measured thought a load cell. Two linear variable differential transformers (LVDT) are installed vertically, one at each edge of the wall to measure average curvature at wall base. In addition, the test setup includes a vertical accelerometer at each end of the foundation, and an accelerometer measuring longitudinally movement of foundation, in order to measure any possible unwanted base displacement or lifting. An additional accelerometer also measures out-of-plan acceleration on the fourth floor. Instrumentation is schematically shown in Fig. 4a.

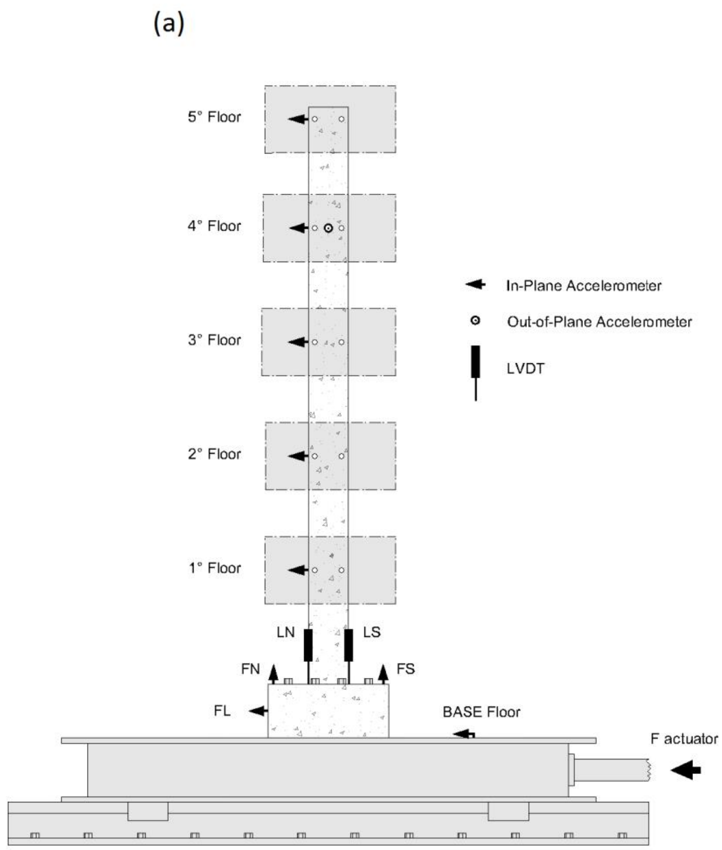

Fig. 4 – Test setup, (a) general view and instrumentation, (b) specimen M1.

4. Test Response

4.1 Failure Patterns

Fig. 5 shows the final stage (after the latest record) of all specimens. Specimens M3 and M4 failed (severe damage that made impossible applying further records) after applying the L150 record, whereas specimen M5 failed with C200. In the case of wall M1 all records were applied without collapse, whereas M2 was only applied up to L100 without collapse, but the test was stop given that risk of collapse. M1 presented horizontal flexural cracks; all of them of minor dimensions except for the one at the wall-foundation interface. Wall M2 presents a similar behavior as M1, except that the main crack changes to the location at the end of the discontinuity region, with minor diagonal cracks. Walls M3 and M4 present loss of concrete cover at the wall-foundation interface. Finally, wall M5 failed frigidly with a large diagonal crack.

4.2 General and amplification results

Main peak results are presented in Table 1. The main parameters under consideration are the peak ground acceleration (PGA), Arias intensity ($I_a = \frac{\pi}{2g}\int_0^t a_g^2(t)dt$, with a_g input acceleration) for the entire input record, Δ_{roof} as the roof displacement (double integration of top), the peak base shear (V_b) and base moment (M_b) determined from the inertial forces measured at each level by accelerometers, and the first (T_1) and second (T_2) mode period measured based on the ratio between the Fourier analysis of the accelerations at each level and the acceleration at the base (forcing action). All those experimental parameters were determined from the measured acceleration with a sampling of 200Hz and filtered with a Butterworth filter (order 4).

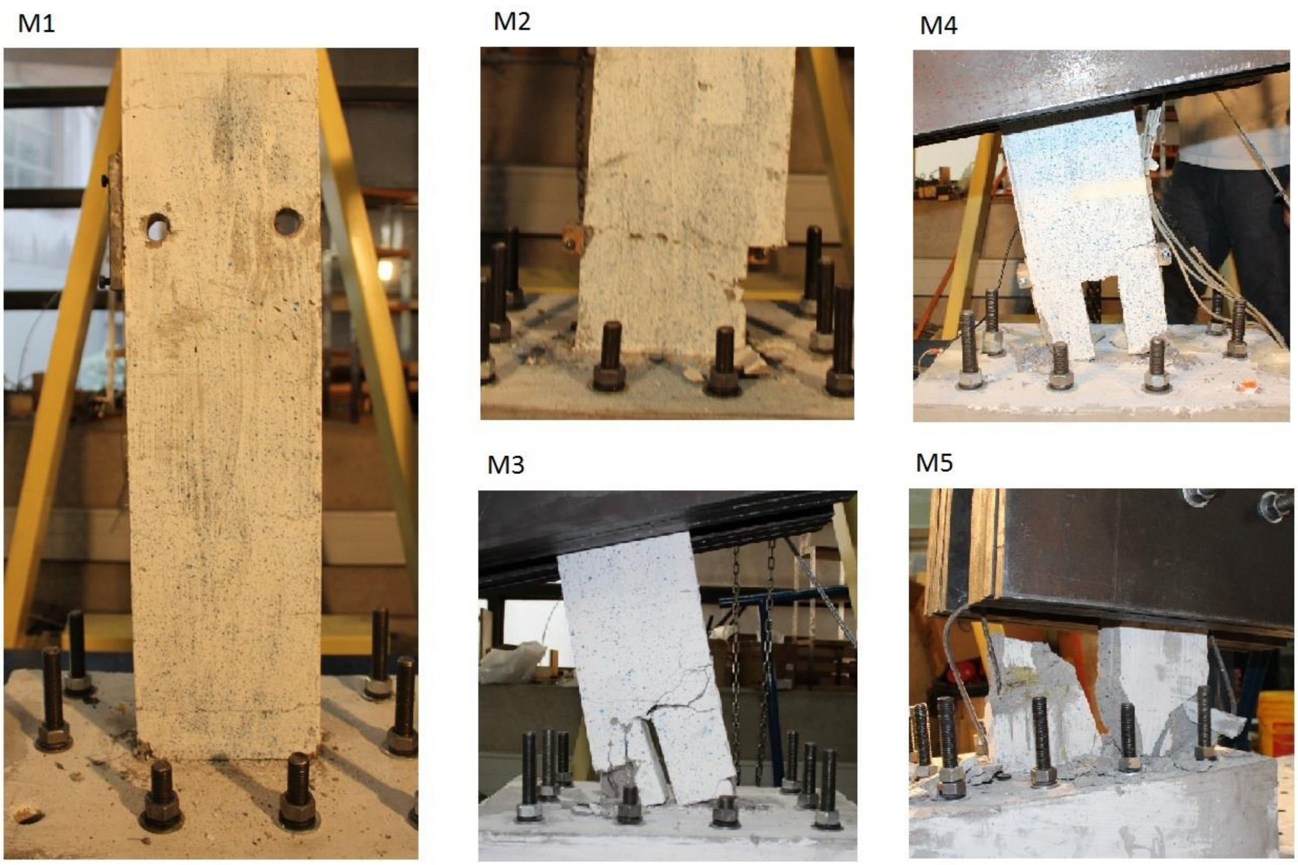

Fig. 5 – Final state of base in test specimens.

According to Table 1, the periods T1 and T2 measured for the record C010 for walls M1, M5, M3 and M4 are 0.53 ± 0.04 s and 0.086 ± 0.003 s, while for M2 are 0.46 and 0071 s respectively, which indicates that the effective stiffness is 0.50 ± 0.08 EI_g. For C100 to C200 records, T1 is 0.93 ± 0.13 s (except for wall M2) with low variability, indicating that the results are comparable for this parameter. This period is consistent with an effective stiffness of 0.16 ± 0.04 EI_g. The maximum roof displacement demand increases moderately between C100 and C200, which means that there is a small increase in ductility, despite the larger intensity of the earthquake. In contrast, L100 and L150 present larger displacement demands, which is consistent with the spectrum (Fig. 3b). The peak base moment for C100 to C200 records is maintained in a range of 3.17 ± 0.32 kN·m, which is close to the moment capacity of 3.47 kN·m (My = 3.2 kN·m), indicating a plastic hinge has been formed. The larger displacement (ductility) demands of L100 and L150 records, results in an increase of the base moment, especially in the case of collapse. Base shear has sustained increments for records C010 to C200, whereas for records L100 and L150 it decreases, since the records are not rich in high frequency contents.

The little correlation between the base shear and the roof displacement, as shown in Fig. 6d for M1 under C200 record, denotes the important influence of the higher modes shear, while for the base moment, plotted in Fig. 6c, the response is much more dependent on the roof displacement, i.e. the first mode. By observing the height (location) of the resultant equivalent lateral force at maximum base shear in Fig. 7, in the case of C010 it reaches 0.46 ± 0.06 in all walls of the total height (h_w) wall. For records C100 to C200 there is progressive increase in the maximum base shear, which corresponds to a lower resultant lateral force, starting at 0.38 ±

$0.02h_w$ ($0.31\ h_w$ for M2) and going as low as $0.18 \pm 0.02h_w$ ($0.12\ h_w$ for M4). While for L100 record it reaches $0.61 \pm 0.07h_w$ (similar to consider force profile for the horizontal forces as an inverted triangle) those results are so similar in all walls. Equivalent forces applied at low height, as seen between C100 and C200 indicates involvement of higher modes, since the base of the wall has reached its moment capacity amplifying the base shear. The envelope of shear force for wall M1 is shown in Fig.6b, and indicates an increase of shear between levels 3 and 4 in the records C100 to C200, expected when a second mode is active, and is not observable for other records where shear increases, shear decreases in level 2 and 3 according inflection of the second mode in this level. Something similar occurs with the base moment envelope for wall M1 (Fig. 5(a)), where over 50% of base moment is maintained up to level 3 in C100 to C200, whereas for the rest (L100 and L150) the remaining moment drops below half at mid-height.

Table 1 – Peak response for tests.

Muro/ registro		PGA (g)	Ia (g·s)	Δroof (mm)	Vb (kN)	Mb (kN·m)	T1 (s)	T2 (s)
M1	C010	0.06	0.0031	2.6	0.26	0.30	0.56	0.09
	C100	0.65	0.57	55	3.73	3.34	0.87	0.12
	C130	0.84	0.94	60	3.87	2.93	0.91	0.13
	C150	0.98	1.25	63	4.21	3.24	0.94	0.14
	C200	1.13	2.07	76	4.97	3.32	0.99	0.13
	L100	0.48	0.65	129	2.60	3.75	1.14	0.14
	L150	0.62	1.35	200	3.10	3.80	1.41	0.14
M2	C010	0.06	0.0022	1.9	0.24	0.29	0.46	0.07
	C100	0.74	0.62	45	3.17	3.29	0.85	0.09
	C130	0.94	0.99	62	3.96	2.77	0.99	0.10
	C150	1.03	1.30	83	3.44	3.09	1.06	0.10
	C200	1.24	2.18	115	5.04	3.15	1.34	0.10
	L100	0.47	0.65	209	2.36	3.63	1.67	0.11
M3	C010	0.05	0.0017	2.0	0.23	0.24	0.50	0.09
	C100	0.72	0.57	54	4.29	3.48	0.82	0.12
	C130	0.87	0.96	62	4.85	3.33	0.87	0.12
	C150	1.23	1.23	63	5.10	3.29	0.90	0.13
	C200	1.26	2.13	72	5.36	3.37	0.95	0.13
	L100	0.47	0.67	131	2.88	4.09	1.08	0.14
	L150*	1.09	0.99	182	3.98	5.70	1.20	0.14
M4	C010	0.01	0.0001	0.8	0.07	0.08	0.48	0.08
	C100	0.62	0.50	54	3.79	3.26	0.87	0.12
	C130	0.83	0.85	55	3.53	2.84	0.93	0.13
	C150	0.95	1.11	58	4.08	3.24	0.95	0.13
	C200	1.10	1.84	73	5.16	3.59	1.00	0.14
	L100	0.51	0.62	119	2.48	3.73	1.26	0.13
	L150*	0.80	0.61	191	4.00	4.97	1.20	0.14
M5	C010	0.05	0.0016	1.7	0.21	0.19	0.54	0.08
	C100	0.74	0.62	53	3.55	3.27	0.80	0.11
	C130	0.93	1.04	60	4.30	3.00	0.88	0.12
	C150	1.07	1.33	58	4.79	2.93	0.92	0.12
	C200*	1.10	1.07	61	4.17	2.86	0.96	0.13

*: Specimen Collapse.

In order to compare the experimental base shear, a spectral modal analysis (ME) and a linear time-history analysis (THL) are performed, both with a modal damping ratio of 5% and using the actual input (record) of each test. The ME is the preferred model for design of RC structures and using a sufficient number of modes (generally exceeding 90% of the equivalent mass) linear effects of higher modes are captured; in this case five modes are used. In the other hand, THL is considered a better approach to capture the dynamic behavior, although nonlinear behavior is not included. Besides of using two benchmarks analysis, for comparison purposes, maximum base moment and shear (1 peak) together with an average of the largest 10 peak values are also used for base shear and moment, in order to observe whether conclusions are derive not only for one specific point (peak). Additionally, the dynamic amplification factor (ω_V) is defined as the ratio between the experimental shear to moment ratio (V_{exp}/M_{exp}) to the same ratio determined for the models (V_L/M_L), to capture the amplification due to flexural yielding, as $\omega_V = \frac{V_{EXP}}{M_{EXP}} / \frac{V_L}{M_L}$.

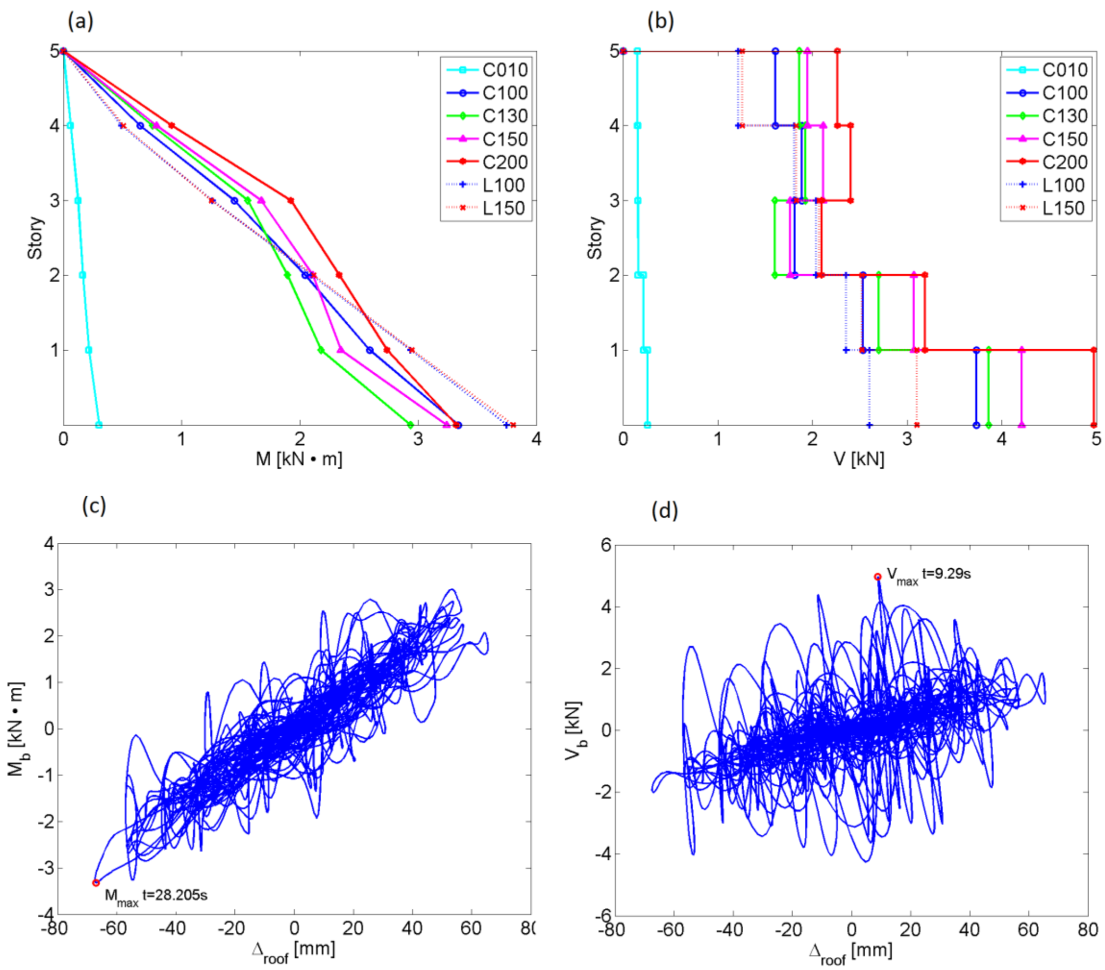

Fig. 6 – Wall M1 - (a) moment envelop distribution, (b) shear envelop distribution, (c) moment vs. top displacement for C200, and (d) shear vs. top displacement for C200.

The dynamic amplification of shear achieved in all tests is shown in Fig. 8. Amplification for record C010 is close to 1 (i.e., not amplified), with a better correlation with THL for 10 peaks (Fig. 8d). Both results are expected since the specimen is maintained in the linear range being THL a better model approximation. Amplification gradually increases from C100 to C200, C100 presenting mean amplification of 1.32 and C200 of 1.80, compared to THL model and using 10 peaks mean. L100 and L150 present low amplification with values close to 1.1 and 1.2, respectively. Note that the scatter showed between the different specimens reduces by considering the THL analysis with 10 peak values.

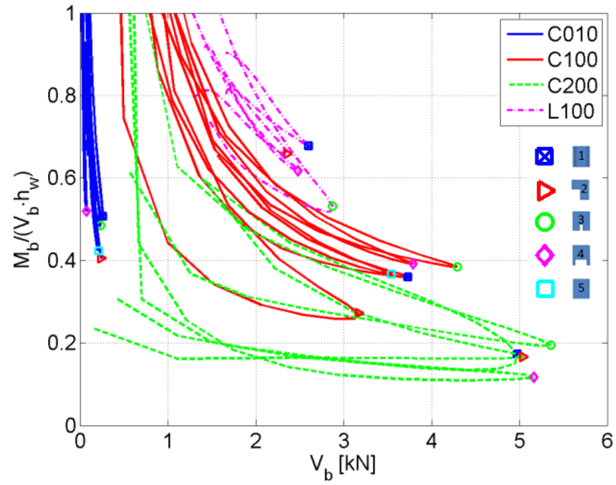

Fig. 7 Force resultant height versus base Shear for in walls – close to maximum base shear.

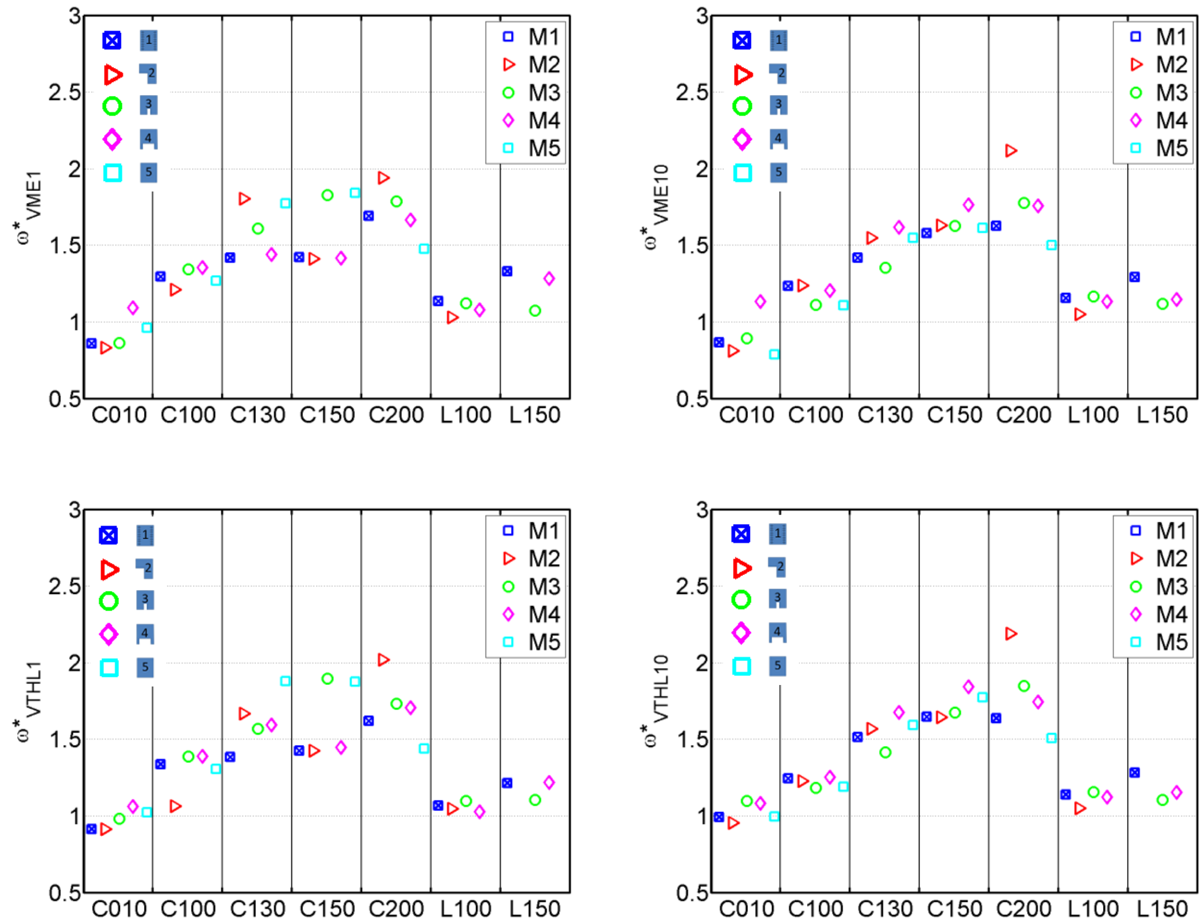

Fig. 8 Shear dynamic amplification based on (a) ME and 1 peak, (b) ME and 10 peak values, (c) THL and 1 peak, and (d) THL and 10 peak values.

Fig. 9a shows the amplification versus the top displacement. Although there is correlation between those variables for a specific record, they do not correlate for different records (Constitución and Llolleo records are linked by a dot line). Despite this, it is interesting to note that the curves for walls with central opening (M3, M4), tend to be above the continuous walls; except for M2 that presents a different behavior due to its different period. In the other hand, a good correlation between the amplification and Arias intensity (Ia) is observed in Fig 9b.

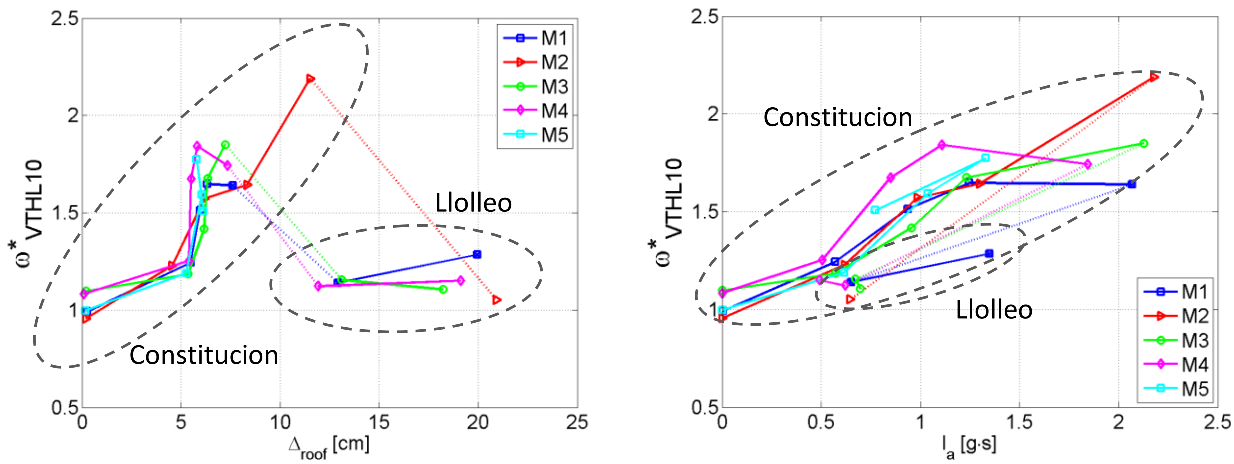

Fig. 9 Dynamic shear amplification versus (a) roof displacement and (b) Arias Intensity (THL 10 peaks).

4. Conclusions

The dynamic amplification factor of shear obtained by comparing a linear model varies with the type of earthquake (frequency content and intensity) and the natural period of the structure. This is consistent with a decrease of the height of the resultant forces. Besides, the amplification results indicate that considering 1 or 10 peaks for the analysis, yield similar results.

Failure modes were different for different specimens, presenting more diagonal cracks in cases with discontinuities. However, no significant influence is observed in shear amplification in walls having a central opening at the base, regardless of whether this is 10% or 30% of total length. It is explained throw small differences between natural periods and height of equivalent lateral force at maximum shear in specimens, in addition, failure just influence structural behavior at the specific instant (quiero decir que la falla solo influye en la respuesta en el momento que esta ocurre). In the case of flag-type discontinuity, changing stiffness (or period) seems to be more relevant regarding the shear amplification.

Ductility demands shows no direct correlation with amplification when looking into 2 different earthquakes that are amplified, whereas the frequency content and Arias intensity (Ia) of the record affect the amplification.

Acknowledgements

This study was financially supported by Chile's National Commission on Scientific and Technological Research (CONICYT) under the project Fondecyt 2013, Regular Research Funding Competition under Grant No. 1130219. The contribution by prof. Fabián Rojas with the synthetic record generation is also acknowledged.

5. References

[1] Blakeley, R., Cooney, R. & Megget, L. (1975): Seismic Hear Loading at Flexural Capacity in Cantilever Wall Structures. *Bulletin of the New Zeland National Society for Rarthquake Engineering, Vol. 8, NO. 4. December 1975*, pp. 278-290.

[2] NZS (1982) NZS 3101: Part 1, Concete Structures Standard; Part 2, Commentary on the design of concrete structures, New Zealand Standards, Wellington.

[3] Derecho, A. & Corley, W. (1984): Design requierements for structural walls in multystory buildings. 8th World Conference on Earthquake Engineering, vol. 5 San Francisco.

[4] Keinzel, E. (1984) Ductility requirements for shear wall structures in seismic areas. 8th World Conference on Earthquake Engineering, San Francisco, CA, Vol. 5.

[5] Kabeyasawa, T. & Ogata, K. (1984): Ultimate-state design of RC wall-frame structures. Trans Jap Conc Inst 6:629-636.

[6] Eibl J, Keinzel E (1988) Seismic shear forces in RC cantilever shear walls, vol VI. 9th World Conference on Earthquake Engineering, Tokyo-Kyoto

[7] Keintzel E (1990) Seismic design shear forces in reinforced concrete cantilever shear wall structures. Eur J Earthq Eng 3:7–16.

[8] Pennucci D, Sullivan, TJ, Calvi GM (2010) Evaluation of higher mode effects in tall building response. 14th European Conference Earthquake Engineering, Ohrid.

[9] Fischinger M, Rejec K, Isakovic T (2010) Shear magnification factors for RC Structural Walls in Eurocode 8. 14th European Conference on Earthquake Engineering, Ohrid.

[10] Rutemberg, A. (2013): Seismic shear forces on RC walls: review and bibliography. Bull Earthquake Eng (2013) 11:1727-1751.

[11] Panagiotou M, Restrepo JI (2007) Lessons learnt from the UCSD full-scale shake table testing on a 7-story residential building. SEAOC Convention, Squaw Creek.

[12] Ghorbanirenani, I., Tremblay, R., Léger, P., ASCE, M. & Leclerc, M. (2012): Shake Table Testing of Slender RC Shear Wall Subjected to Eastern North America Seismic Ground Motions. Journal of Structural Enginerring Vol. 138, No. 12, December 1, 2012.

[13] Martinelli, P. & Filippou F. (2009): Simulation of the shaking table test of a seven-story shear wall building. Earthquake Eng. Struct. Dyn., 38(5), 587-607.

[14] Luu, H., Ghorbanirenani, I., Léger, P. & Tremblay, R. (2011): Structural dynamics of slender ductile reinforced concrete shear walls. 8th International Conference of Struct Dyn, EURODYN 2011, Leuven, Belgium, pp. 355-362.

[15] Isakovic, T., Eser, N. & Fischinger, M. (2016): Inelastic shear response of RC coupled structural walls. New Zealand Society for Earth. Eng. (NZSEE) 2016 Conference.

[16] MINVU (2011): DS 61 - Seismic structures design (in spanish). Ministry of Housing and Urban Development, Santiago, Chile.

[17] INN (2012): *NCh433 Of.1996 - Seismic structures design.* (in spanish). s.l.:National Standards Institute, Chile.

[18] ACI (2008): *318 - Regulation Requirements for Structural Concrete.* s.l.:American Concrete Institute.

[19] Lagos, R., Kupfer, M., Lindenberg, J., Bonelli, P., Saragoni, R., Guendelman, T., Massone, L., Boroschek, R. & Yañez, F. (2012): Seismic Performance of Hig-rise Concrete Buildings in Chile. International Journal of High-Rise Buildings, September 2012, Vol 1, No 3.

[20] Carvalho, E., 1998. Seismic testing of structures. 11° European Conference on Earthquake Enfineering. Rottedam: Balkema, pp. 53-64.

[21] Kent, D.C. and Park, R. (1971): Flexural members with confined concrete. ASCE Journal of the Structural Division 97(7): 1969-1990.

[22] Mander, J.B., Priesley, M.J.N. & Park, R. (1984): Seismic design of bridge piers. Research Rep. No. 84-2, Dept of Civil Engineering, Univ. of Canterbury, Chistchurch, New Zeland.